2026 International Conference on Computing, Networking and Communications (ICNC): Next generation of mobile networks (6G and beyond)

Distributed Cooperative Downlink for NextG Mobile Networks

Yibin Liang, Usama Saeed, Yang (Cindy) Yi, and Lingjia Liu

***Abstract*—Distributed multiple-input multiple-output (D-MIMO) offers a pathway to achieve massive MIMO gains while mitigating the physical constraints of co-located antenna arrays. However, the reliance on fiber connections for distributed radio units restricts deployment flexibility and elevates infrastructure expenses. To address these limitations, mobile D-MIMO (MD-MIMO) was recently introduced, an innovative extension where distributed antenna arrays connect wirelessly to the base station, and all radio nodes possess mobility. We present a novel MD-MIMO architectures for cooperative downlink communication, detailing the system design and key enabling technologies, such as MIMO precoding and channel prediction. Performance evaluation using realistic 3GPP mobile channel models demonstrates the significant potential of the proposed MD-MIMO system to enhance network throughput and reliability.**

***Index Terms*—Wireless, Mobile Networks, Distributed MIMO.**

I. Introduction

Multiple-input multiple-output (MIMO) significantly enhanced capacity and reliability in 4G networks, paving the way for 5G's massive MIMO [1] to further boost network performance. However, the physical limitations of deploying numerous antennas at a single base station constrain achievable gains. To address this, distributed MIMO (D-MIMO) has emerged as a promising architecture where geographically separated radio units (RUs) collaborate to serve users through joint transmission or cooperative reception. Evolving from 4G's Coordinated Multi-Point transmission (CoMP) [2] and refined by techniques like joint transmission with channel feedback [3] and advanced beamforming, this concept has been integrated into 5G New Radio (NR) standards as multiple Transmission and Reception Point (mTRP) [4].

Nevertheless, the need for mobile D-MIMO (MD-MIMO) arises from several key challenges and evolving demands in wireless communication networks, particularly as we move towards next generation (NextG) networks [5]. We refer to MD-MIMO as an evolution of D-MIMO that allows all nodes, including the base station, to be mobile or portable, thereby enabling full control over both micro- and macro-diversity.

In [6], a two-phase coherent joint-transmission scenario is analyzed from a capacity perspective to illustrate the capacity trade-off inherent in MD-MIMO network topology. Building upon the MD-MIMO concept introduced in [5] within the context of 3GPP standards, we note that few prior works have thoroughly addressed the associated design challenges. To this end, we introduce a novel MD-MIMO architecture design for distributed cooperative downlink (DC-DL). We present detailed system and algorithm designs, along with comprehensive performance evaluations using realistic 3GPP mobile channel models for different scenarios.

Prior work has explored cooperative distributed antenna systems [7]–[9]. However, our work distinguishes itself by emphasizing novel algorithm designs that confront the critical challenges due to the mobility of both the gNB and RUs – a significant aspect not thoroughly investigated previously.

The remainder of this article is structured as follows: Section II reviews existing D-MIMO technologies and highlights the core challenges in their extension to MD-MIMO. We then present a detailed description of the proposed MD-MIMO architecture and key algorithm designs in Section III. Section IV follows with comprehensive system-level simulation results across diverse mobile scenarios and analyzing the trade-offs between reliability and capacity. Finally, Section V concludes the current work and outlines future research directions.

II. MD-MIMO Overview

Distributed MIMO operation refers to a range of techniques wherein multiple geographically distributed radio nodes collaborate to facilitate data transmission between source and destination nodes, as illustrated in Figure 1. We provide a concise review of recent progress in D-MIMO, particularly within the context of 3GPP standards, and highlights the critical technical challenges for its extension to MD-MIMO.

A key advantage of D-MIMO over co-located MIMO is its ability to enable flexible MIMO operation,including joint transmission [10] and interference coordination [11], while circumventing the physical size constraints at the base station [8]. Achieving independent channel realizations in sub-6 GHz bands requires antenna spacing of at least a half wavelength, which can be spatially and economically prohibitive. In contrast, the unconstrained geographical distribution of D-MIMO nodes provides macro diversity, mitigating large-scale fading and shadowing [12].

In the context of 5G networks, Remote Units (RUs) capable of coherent joint transmission can function as a large virtual antenna array, enhancing spatial multiplexing and antenna diversity. Simpler D-MIMO approaches, such as Distributed Antenna Systems (DAS) and Dynamic Point Selection (DPS), leverage macro diversity from geographically dispersed RUs to

Efforts sponsored by the U.S. Government under the Training and Readiness Accelerator II (TReX II), OTA. The U.S. Government is authorized to reproduce and distribute reprints for Governmental purposes notwithstanding any copyright notation thereon. The views and conclusions contained herein are those of the authors and should not be interpreted as necessarily representing the official policies or endorsements, either expressed or implied, of the U.S. Government.

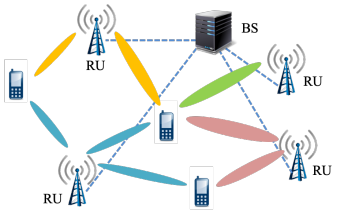

Fig. 1. Illustration of a distributed MIMO network

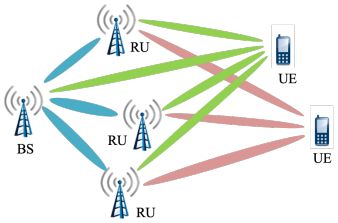

Fig. 2. Distributed cooperative downlink Scenario

improve coverage [13]. Joint Transmission Coordinated Multi-Point (JT-CoMP) [2] takes advantage of coherent transmission from multiple nodes to create a large virtual array, exploiting channel micro diversity [9]. Recent years have witnessed successful experimental demonstrations of coherent D-MIMO operation [14], with commercial entities also showcasing high-performance D-MIMO prototypes [15]. Looking ahead, cell-free architectures, another promising next-generation technology, will leverage the D-MIMO strategy to enhance system capacity by eliminating inter-cell interference through coherent cooperation among distributed nodes [16], [17].

The significant potential of MD-MIMO is accompanied by several design and implementation challenges. Overcoming wireless front-haul bandwidth limitations, a consequence of replacing wired connections, requires sophisticated MIMO precoding, efficient data sharing strategies, and reduced control overhead. The reliable frequency and timing synchronization offered by fiber must be replicated through new protocols and algorithms suitable for wireless RUs. Moreover, adapting to the dynamic distributed MIMO channels necessitates improving conventional precoding and detection techniques, with channel prediction becoming a prerequisite for good performance and lower feedback. Lastly, the distributed mobility of nodes necessitates the development of new cooperative transmission and reception algorithms.

Realizing the proposed MD-MIMO designs requires several critical algorithms that extend existing methods for D-MIMO systems. We detail critical system design aspects, including network topology, transmission and reception procedures, channel estimation/prediction, and precoding for the DC-DL in Section III. We briefly discuss performance trade-offs from an algorithm design perspective, with system-level performance evaluation presented in Section IV.

III. Distributed Cooperative Downlink

To extend D-MIMO to MD-MIMO for multi-user scenarios, we propose a novel architecture for distributed cooperative downlink (DC-DL). In distributed downlink scenarios, UEs at the cell edge often experience degraded transmission/reception performance due to weak signals or blockage. Employing distributed RUs and the gNB for cooperative transmission can enhance the reliability and throughput for these UEs.

The downlink transmission follows a two-phase procedure as illustrated in Figure 2. In phase-1, the gNB broadcasts the user data to participating RUs, and in phase-2 the gNB and RUs can form a coherent distributed array to simultaneously transmit user data to multiple destination UEs.

In phase 1, the gNB can leverage the standard physical downlink shared channel (PDSCH) to simultaneously broadcast data to multiple participating RUs. For phase 2, the RUs can extend PDSCH for this purpose.

The channels from the gNB to multiple RUs form a broadcast channel, where the capacity is limited by the lowest rate among the receiving RUs. Consequently, careful selection of participating RUs is necessary; including more RUs for the first transmission phase can reduce overall throughput. Conversely, the aggregate throughput of the second transmission phase typically increases with more transmitting RUs. Optimal transmitting node selection is coupled with the precoding procedure in both phases, making it difficult to achieve. In this work, we decouple the node selection process from the precoding algorithm design and use the channel quality indicator (CQI) for selecting the best transmitting nodes.

Although a precoding strategy that accounts for both common information in phase one and multi-user precoding in phase two is crucial for maximizing the capacity, it unfortunately results in a non-convex optimization problem, complicating numerical solutions. In [18], a distributed precoding algorithm is presented to decompose the optimization problem into a sequence of convex subproblems.

Effective precoding for joint transmission for both phases demands channel state information (CSI) for all distributed links. After the gNB collects the CSI and compute the precoding matrices for both transmission phases, it sends then to the RUs for distributed signal processing. Participating RUs, chosen by the gNB based on connection quality, can provide CSI feedback for the gNB-RU links. For the RU-UE and gNB-UE links, two feedback mechanisms are possible: direct reporting from the UEs or relaying the information via the RUs, with the latter introducing a substantially greater delay.

The considerable number of distributed links introduces a substantial overhead associated with CSI feedback, presenting a significant design challenge. Additionally, the inherent delays between CSI feedback acquisition and precoding matrix application often cause the CSI to become stale in rapidly evolving network topologies. Consequently, the gNB is required to implement channel prediction to sustain acceptable precoding performance.

A. Precoding for Broadcast Data

The gNB S broadcasts the same data to all its associated UEs in preparation for the coherent joint transmission in forwarding phase which requires that all nodes in the set

$\{\mathcal{U}_S, S\}$ have the same data $\mathbf{x}$. Each node $\mathcal{U}_S(i)$ receives a signal $\mathbf{y}_{\mathcal{U}_S(i)}$ as

$$\mathbf{y}_{\mathcal{U}_S(i)} = \mathbf{H}_{\mathcal{U}_S(i),S}\mathbf{P}_S\mathbf{x} + \mathbf{n}_{\mathcal{U}_S(i)} \tag{1}$$

$\mathbf{H}_{S,\mathcal{U}_S(i)} \in \mathbb{C}^{N_U \times N_g}$ denotes the channel between nodes S and $\mathcal{U}_S(i)$, where N_U and N_g are the number of antennas at a user node and the transmit squad gNB node, respectively, $\mathbf{x} \in \mathbb{C}^{l\times 1}$ is the information symbols vector, $\mathbf{P}_S \in \mathbb{C}^{N_g \times l}$ is the precoder matrix that can be designed to accommodate $l \leq N_U$ spatial streams since it is assumed that $N_U < N_g$, and noise is denoted by $\mathbf{n}_{\mathcal{U}_S(i)} \in \mathcal{N}(\mathbf{0}, \boldsymbol{\sigma}^2_{\mathcal{U}_S(i)})$ where $\boldsymbol{\sigma}^2_{\mathcal{U}_S(i)} = \mathbb{E}\left(\mathbf{n}_{\mathcal{U}_S(i)}\mathbf{n}^H_{\mathcal{U}_S(i)}\right)$ is the noise covariance matrix.

The collective channel $\mathbf{H} = [\mathbf{H}^T_{S,\mathcal{U}_S(0)}, .., \mathbf{H}^T_{S,\mathcal{U}_S(|\mathcal{U}_S|-1)}]^T$ represents a MIMO broadcast channel with common information (MIMO-BC) [19]. The precoder $\mathbf{P} \in \mathbb{C}^{N_g \times l}, l \leq N_U$ design criterion to maximize the probability of data arriving intact at *all* nodes in $\mathcal{U}_S$, with minimum error correction coding overhead. To do so, the objective function is chosen to ensure a minimum level of performance for the worst case node, which can be formulated in terms of the following max-min optimization problem [20].

$$\begin{aligned} \max_{\mathbf{Q}_S} \min_{i\in\{0,..,|\mathcal{U}_S|-1\}} \quad & \log|\mathbf{I}_{N_U} + \boldsymbol{\sigma}^{-2}_{\mathcal{U}_S(i)}\mathbf{H}_{\mathcal{U}_S(i),S}\mathbf{Q}\mathbf{H}^H_{\mathcal{U}_S(i),S}| \\ \text{s.t.} \quad & \text{tr}(\mathbf{Q}) \leq P_t \\ & \text{rank}(\mathbf{Q}) \leq N_U \end{aligned} \tag{2}$$

where P_t denotes the maximum transmit power of the gNB.

The solution $\mathbf{Q}$ is then factorized into $\mathbf{P}\mathbf{P}^H$ to find the required precoder. We note that the second constraint makes the optimization problem non-convex. Relaxing the problem by ignoring this constraint, the problem becomes convex and the unique solution is found. Now we satisfy the second constraint by selecting the $N_g \times l$ sub-matrix from the solution $\mathbf{P}$ that maximizes the given objective function.

B. ML-based Channel Prediction

The large number of antenna elements in MD-MIMO systems introduces substantial challenges for channel estimation and feedback. Although 3GPP standards provide downlink channel estimation procedures and codebook-based CSI feedback mechanisms to mitigate overhead [21], the necessary codebook size scales exponentially with the number of transmit antennas, making frequent CSI feedback impractical.

Several machine learning-based techniques, such as CSI compression [22], optimized codebook design [23], and channel prediction [24], have been explored to mitigate these challenges. However, these methods typically require extensive offline training, and any statistical mismatch for real-time channel conditions can severely impair performance [25].

Addressing the challenges of CSI feedback overhead in MD-MIMO necessitates machine learning techniques capable of online, adaptive reduction. Reservoir computing (RC), a particular class of recurrent neural networks (RNNs), has recently emerged as a potent methodology for addressing problems in wireless communications in an online and real-time fashion. RC-based methods have demonstrated effectiveness in wireless communication tasks such as symbol detection [26], showcasing their ability to learn spatio-temporal correlations. This lightweight training makes RC highly adaptable to dynamic environments [27], positioning it as a strong candidate for online channel prediction within MD-MIMO systems.

An Echo State Network (ESN) is a specific kind of RC, which consists of an input layer, a recurrent reservoir layer, and an output layer, as shown in Figure 3. The input and reservoir layers are fixed and randomly initialized while only the weights of the output layer are trained. This makes the training of ESNs simple and fast, making them ideal for high-speed applications such as communication systems. We construct an ESN-based channel prediction algorithm which makes predictions using limited training data.

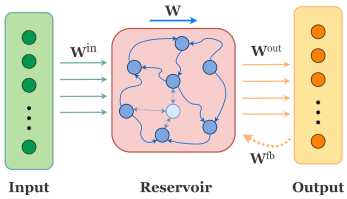

Fig. 3. ESN reservoir structure

The internal state of an ESN with N neurons in the reservoir, $\boldsymbol{s}(t) \in \mathbb{C}^{N\times 1}$, is given by:

$$\boldsymbol{s}(t) = f\left(\boldsymbol{W}\boldsymbol{s}(t-1) + \boldsymbol{W}_{in}\bar{\mathbf{H}}(t)\right), \tag{3}$$

where $\boldsymbol{s}(-1)$ is initialized as a zero vector, $f(\cdot)$ is the activation function, $\boldsymbol{W} \in \mathbb{C}^{(N\times N)}$ is the reservoir weight, $\boldsymbol{W}_{in} \in \mathbb{C}^{(N\times N_{sc})}$ is the input weight matrix and $\bar{\mathbf{H}}(t) \in \mathbb{C}^{N_{sc}\times 1}$ is the channel for each OFDM symbol with N_{sc} subcarriers. The output of the ESN is expressed as:

$$\hat{\boldsymbol{x}}(t) = f_{out}(\boldsymbol{W}_{out}\boldsymbol{z}(t)), \tag{4}$$

where $f_{out}(\cdot)$ is the activation function for the output layer, $\boldsymbol{W}_{out} \in \mathbb{C}^{N_{sc}\times(N+N_{sc})}$ is the output weight matrix and $\boldsymbol{z}(t) = [\boldsymbol{s}(t)^T, \bar{\mathbf{H}}(t)^T]^T \in \mathbb{C}^{(N+N_{sc})\times 1}$ is the concatenation of the internal state and the input. The only trainable weights are the output weights, which are learned through a closed-form least-squares solution which aims to minimize the mean square error between the output $\hat{\boldsymbol{x}}(t)$ and the intended output $\boldsymbol{x}(t)$. The regression procedure can be defined as:

$$\begin{aligned} \hat{\boldsymbol{W}}_{out} &= \arg\min_{\boldsymbol{W}_{out}} \sum_{t=0}^{N_{train}} ||\hat{\boldsymbol{x}}(t) - \boldsymbol{x}(t)||_2^2 \\ &= \arg\min_{\boldsymbol{W}_{out}} ||\hat{\boldsymbol{x}} - \boldsymbol{x}||_F^2 \end{aligned} \tag{5}$$

where N_{train} is the number of OFDM symbols used for training, $\hat{\boldsymbol{x}} = [\hat{\boldsymbol{x}}(0), \hat{\boldsymbol{x}}(1), \cdots \hat{\boldsymbol{x}}(N_{train}-1)] \in \mathbb{C}^{N_{sc}\times N_{train}}$ and $\boldsymbol{x} = [\boldsymbol{x}(0), \boldsymbol{x}(1), \cdots \boldsymbol{x}(N_{train}-1)] \in \mathbb{C}^{N_{sc}\times N_{train}}$ are the concatenation of the output signal and target transmit signal

matrices, respectively. In the training period, the concatenated vector $\boldsymbol{z}(t)$ is recorded and forms the following matrix:

$$\boldsymbol{Z} = [\boldsymbol{z}(0), \boldsymbol{z}(1), \cdots, \boldsymbol{z}(N_{train}-1)] \in \mathbb{C}^{(N+N_{sc})\times N_{train}} \tag{6}$$

The least square solution assuming linear activation is:

$$\hat{\boldsymbol{W}}_{out} = \boldsymbol{x}\boldsymbol{Z}^{\dagger}, \tag{7}$$

where $\boldsymbol{Z}^{\dagger}$ is the Moore-Penrose pseudo inverse of $\boldsymbol{Z}$. In this work, we adopt (7) to compute $\hat{\boldsymbol{W}}_{out}$, despite employing a nonlinear activation function as it offers a low-complexity approximation with good empirical performance.

IV. Performance Evaluation

In this section, we present preliminary performance evaluation for the introduced MD-MIMO architectures. We evaluate bit error rates (BER) and throughput performance in different scenarios and analyze the trade-off for system reliability and capacity. We also highlight the performance improvement with ML-based channel prediction as compared with conventional methods. The simulation parameters for the following evaluations are summarized in Table I.

TABLE I
Simulation Parameters for Distributed Downlink

System Parameters	Values
Center Frequency	2.5 GHz
Subcarrier Spacing	15 kHz
Number of Subcarriers	512
gNB Antennas (Tx/Rx)	4
UE Antennas (Tx/Rx)	2
gNB Transmit Power	35 dBm
UE Transmit Power	26 dBm

The network performance is evaluated under three different scenarios with different mobility settings, as listed in Table II. For each scenarios, multiple random topologies are used to generate Monte-Carlo simulation results. We utilize the 3D Spatial Channel Model frameworks developed by 3GPP for New Radio (NR). These models, grounded in geometry-based stochastic principles, address channel characteristics across both standard cellular environments, as specified in TR 38.901, and vehicular contexts as outlined in TR 37.885.

TABLE II
Mobility Scenarios for Performance Evaluation

Mobility	gNB ground speed	UE relative speed
Low	0.5 km/h	0.05 km/h
Medium	5.0 km/h	0.5 km/h
High	20.0 km/h	2.0 km/h

Figure 4 presents the average downlink throughput for three distinct mobility scenarios. In all tests, we used a fixed number of 6 RUs besides the gNB for cooperative transmission. Throughput was maximized by adaptive modulation and coding schemes (MCS) and scheduling transmissions to UEs with the best channel conditions. For comparison, we use the direct gNB to UE link without additional RUs as the baseline.

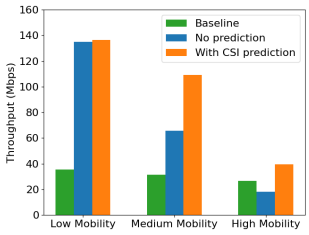

Fig. 4. Average downlink throughput in different mobility scenarios

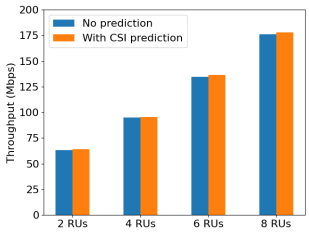

Fig. 5. Average downlink throughput in low mobility scenarios

As the summary indicates, average throughput drops considerably with higher mobility when channel prediction is absent. A critical reason for this is poor precoding performance caused by outdated CSI. Notably, implementing channel prediction allows the distributed downlink scheme to achieve substantial improvements in medium and high mobility scenarios.

To assess the impact of RUs, we evaluated average throughput with varying numbers of RUs. As Figure 5 illustrates, increasing the number of RUs generally improves throughput by effectively leveraging spatial multiplexing gains. However, these gains are difficult to achieve with outdated Channel State Information (CSI), which consistently reduces achievable throughput in medium and high mobility scenarios, as shown in Figure 6 and 7. Therefore, accurate CSI via channel prediction is essential to maintain performance.

To further analyze the effects of mobility, Figure 8 displays the average uncoded and LDPC-coded BER for the distributed

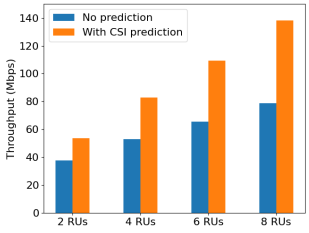

Fig. 6. Average downlink throughput in medium mobility scenarios

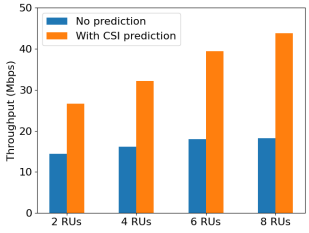

Fig. 7. Average downlink throughput in high mobility scenarios

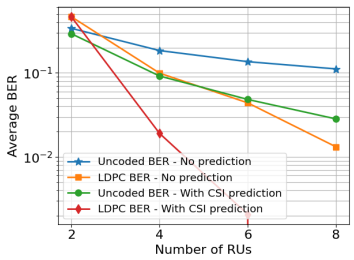

Fig. 8. Average uncoded/coded BER in medium mobility scenario

downlink in a medium mobility scenario. We used 16QAM modulation and rate 1/3 LDPC across all runs, maximizing throughput by scheduling transmissions to UEs with optimal channel conditions. With channel prediction, increasing the number of RUs significantly reduces the average BER, which improves both system reliability and throughput.

As shown in Figure 9, channel prediction delivers even more significant performance improvement in high mobility scenarios. For these tests, we used QPSK modulation and rate 1/3 LDPC, maximizing throughput by scheduling transmissions to UEs with optimal channel conditions.

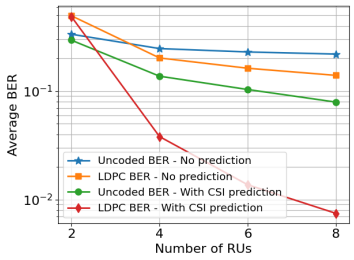

Fig. 9. Average uncoded/coded BER in high mobility scenario

V. Conclusions and Future Work

This paper details the key design aspects of the proposed distributed cooperative downlink architecture for MD-MIMO. We provide comprehensive performance evaluations of enabling technologies like distributed precoding and channel prediction, using realistic 3GPP channel models in different mobility scenarios. Our results demonstrate significant improvements in both reliability and system capacity, underscoring the critical role of channel prediction. Future work will be needed to address the unique design challenges in cooperative uplink scenarios for MD-MIMO.

References

[1] H. Jin, K. Liu, M. Zhang, L. Zhang, G. Lee, E. N. Farag, D. Zhu, E. Onggosanusi, M. Shafi, and H. Tataria, "Massive MIMO evolution toward 3GPP release 18," *IEEE J. Sel. Areas Commun.*, vol. 41, no. 6, pp. 1635–1654, 2023.

[2] M. Sawahashi, Y. Kishiyama, A. Morimoto, D. Nishikawa, and M. Tanno, "Coordinated multipoint transmission/reception techniques for LTE-advanced [Coordinated and distributed MIMO]," *IEEE Wireless Commun. Mag.*, vol. 17, no. 3, pp. 26–34, Jun. 2010.

[3] L. Liu, J. Zhang, B. Clerckx, and J.-K. Han, "Coordinated multipoint (CoMP) joint transmission using channel information feedback and higher rank dedicated beam-forming," May 2013.

[4] W. Chen, X. Lin, J. Lee, A. Toskala, S. Sun, C. F. Chiasserini, and L. Liu, "5G-advanced toward 6G: Past, present, and future," *IEEE J. Sel. Areas Commun.*, vol. 41, no. 6, pp. 1592–1619, 2023.

[5] K. A. Said, Y. Liang, U. Saeed, R. Safavinejad, K. S. Bondada, E. Allen, N. Mohammadi, B. Pimentel, B. Kelley, J. Reed *et al.*, "Mobile distributed MIMO (MD-MIMO) for NextG: Mobility meets cooperation in distributed arrays," *arXiv preprint arXiv:2504.12244*, 2025.

[6] K. S. Bondada, D. J. Jakubisin, K. Said, R. M. Buehrer, and L. Liu, "Wireless mobile distributed-MIMO for 6G," in *Proceedings IEEE 100th Vehicular Technology Conference*, 2024, pp. 1–7.

[7] X.-H. You, D.-M. Wang, B. Sheng, X.-Q. Gao, X.-S. Zhao, and M. Chen, "Cooperative distributed antenna systems for mobile communications [Coordinated and distributed MIMO]," *IEEE Wireless Commun. Mag.*, vol. 17, no. 3, pp. 35–43, Jun. 2010.

[8] S. Ma, Y. Yang, and H. Sharif, "Distributed MIMO technologies in cooperative wireless networks," *IEEE Commun. Mag.*, vol. 49, no. 5, pp. 78–82, 2011.

[9] O. Haliloglu, H. Yu, C. Madapatha, H. Guo, F. E. Kadan, A. Wolfgang, R. Puerta, P. Frenger, and T. Svensson, "Distributed MIMO systems for 6G," in *2023 Joint European Conference on Networks and Communications & 6G Summit (EuCNC/6G Summit)*, 2023, pp. 156–161.

[10] L. Liu and J. Zhang, "System and method for dynamic cell selection and resource mapping for CoMP joint transmission," Sep. 25 2012, uS Patent 8,274,951.

[11] L. Liu, J. Zhang, and Z. Pi, "Inter-cell interference avoidance for downlink transmission," Aug. 2012.

[12] W. Roh and A. Paulraj, "MIMO channel capacity for the distributed antenna," in *Proceedings IEEE 56th Vehicular Technology Conference*, vol. 2, 2002, pp. 706–709 vol.2.

[13] R. Heath, S. Peters, Y. Wang, and J. Zhang, "A current perspective on distributed antenna systems for the downlink of cellular systems," *IEEE Commun. Mag.*, vol. 51, no. 4, pp. 161–167, 2013.

[14] H. V. Balan, R. Rogalin, A. Michaloliakos, K. Psounis, and G. Caire, "AirSync: Enabling distributed multiuser MIMO with full spatial multiplexing," *IEEE/ACM Trans. Netw.*, vol. 21, no. 6, pp. 1681–1695, 2013.

[15] J. Yuan, Y. Liu, Y. Hu, G. Xu, and J. C. Zhang, "Distributed FD-MIMO (D-FD-MIMO): From concept to field test," in *2022 IEEE Radio and Wireless Symposium (RWS)*, 2022, pp. 86–89.

[16] H. He, X. Yu, J. Zhang, S. Song, and K. B. Letaief, "Cell-free massive MIMO for 6G wireless communication networks," *Journal of Commun. and Informat. Netw.*, vol. 6, no. 4, pp. 321–335, 2021.

[17] D. Wang, C. Zhang, Y. Du, J. Zhao, M. Jiang, and X. You, "Implementation of a cloud-based cell-free distributed massive MIMO system," *IEEE Commun. Mag.*, vol. 58, no. 8, pp. 61–67, Aug. 2020.

[18] Y. Li, P. Fan, L. Liu, and Y. Yi, "Distributed MIMO precoding for in-band full-duplex wireless backhaul in heterogeneous networks," *IEEE Trans. Veh. Technol.*, vol. 67, no. 3, pp. 2064–2076, Mar. 2018.

[19] A. Goldsmith, S. Jafar, N. Jindal, and S. Vishwanath, "Capacity limits of MIMO channels," *IEEE J. Sel. Areas Commun.*, vol. 21, no. 5, pp. 684–702, 2003.

[20] M. Razaviyayn, M. Hong, and Z.-Q. Luo, "Linear transceiver design for a MIMO interfering broadcast channel achieving max–min fairness," *Signal Processing*, vol. 93, no. 12, pp. 3327–3340, 2013.

[21] 3GPP, "Study on new radio (NR) access technology; Radio resource control protocol specification (Rel. 16)," in *3GPP TS 38.331*, 2021.

[22] M. B. Mashhadi, Q. Yang, and D. Gündüz, "Distributed deep convolutional compression for massive MIMO CSI feedback," *IEEE Trans. Wireless Commun.*, vol. 20, no. 4, pp. 2621–2633, 2021.

[23] C.-K. Wen, W.-T. Shih, and S. Jin, "Deep learning for massive MIMO CSI feedback," *IEEE Commun. Lett.*, vol. 7, no. 5, pp. 748–751, 2018.

[24] H. Kim, S. Kim, H. Lee, C. Jang, Y. Choi, and J. Choi, "Massive MIMO channel prediction: Kalman filtering vs. machine learning," *IEEE Trans. Commun.*, vol. 69, no. 1, pp. 518–528, 2021.

[25] R. Shafin, L. Liu, V. Chandrasekhar, H. Chen, J. Reed, and J. C. Zhang, "Artificial intelligence-enabled cellular networks: A critical path to beyond-5G and 6G," *IEEE Wireless Commun. Mag.*, vol. 27, no. 2, pp. 212–217, 2020.

[26] Y. Liang, L. Li, Y. Yi, and L. Liu, "Real-time machine learning for symbol detection in MIMO-OFDM systems," in *IEEE INFOCOM 2022 - IEEE Conference on Computer Communications*. London, United Kingdom: IEEE, May 2022, pp. 2068–2077.

[27] J. Xu, Z. Zhou, L. Li, L. Zheng, and L. Liu, "RC-Struct: A structure-based neural network approach for MIMO-OFDM detection," *IEEE Trans. Wireless Commun.*, vol. 21, no. 9, pp. 7181–7193, 2022.